Structure of a Bidisperse Polymer Brush: Monte Carlo Simulation and Self-Consistent Field Results

Pik-Yin Lai* and E. B. Zhulina†

Institut für Physik, Johannes Gutenberg Universität Mainz, Postfach 3980, D 6500 Mainz, Germany

Received October 30, 1991

ABSTRACT: Using the bond-fluctuation model, we perform Monte Carlo simulations for polymer brushes composed of chains of two different chain lengths under good solvent condition. Profiles of monomer density and free end density, chain linear dimensions, and average monomer position along a chain are studied. Quantities measured in the simulations are derived from the analytic self-consistent field (SCF) theory and compared with the simulation data. The structural properties can be quite accurately described by the theory only when both the long and short chains are stretched. In general the predictions from the SCF theory are less satisfactory than in the monodispersed brush. The discrepancies are mainly attributed to the breakdown of the strong stretching condition of the longer chain units in the outer sublayer.

1. Introduction

Grafted chain layers[1,2] (polymer brushes) became the subject of intensive theoretical[3–30] and experimental[31–39] investigations during the last decade due to their wide applications in polymer technology and their importance in understanding the fundamental problems of polymeric materials. Combination of scaling type analysis[3,4] with the more refined self-consistent field (SCF) approach[7,10] made it possible to obtain a detailed picture of the brush structure in a wide range of conditions: in solvents of various strength,[11] in melts and solutions of mobile polymers,[13,14] in charged brushes in dielectric solvents,[15–18] etc. This detailed picture of brush structure comprises the determination of profiles of polymer units and free chain ends in a brush, orientational characteristics of units, distribution of stretching in grafted chains, etc. Unfortunately, experimental observations of brushes available at present are not so sensitive to the details of the structure (such as, for example, distribution of free ends or chain trajectories) but are concerned mainly with more global brush properties, such as brush thickness or force profiles via brush deformation. On the other hand, computer simulations can provide very detailed information from the level of effective monomer to macroscopic quantities. Furthermore approximations in the analytical treatment can be avoided and the system is precisely characterized. Hence some computer simulation studies on polymer brushes including various techniques such as Monte Carlo,[28–30] molecular dynamics,[27] etc. have appeared.

In our previous work,[30] a detailed comparison of SCF theory of the planar monodisperse brush with Monte Carlo (MC) results was carried out. The SCF predictions of a planar brush in athermal solvent were found to be in good agreement with the MC data in a wide range of molecular weights of grafted chains and grafting densities. On the other hand polydispersity can affect the brush structure and its physical properties significantly. For example, a grafted layer composed of chains with uniformly distributed chain lengths is predicted by SCF theory to change the density profile from a convex to a concave one.[19] These effects can probably be tested experimentally by scattering techniques. However, the parameters in many experimental polymer brush systems are not within the range of validity of the analytical SCF theory, such as the chain lengths are finite and/or the grafting densities are not sufficiently high to ensure that all the chains are stretched even in the outer layer. Hence computer simulations are the most appropriate method to obtain information about the brush structure in such situations.

In this paper, we study the case of bidisperse brushes (i.e. brushes consisting of chains of two different lengths) by Monte Carlo simulation of the bond-fluctuation model. SCF theory[19,20] predicts that the equilibrium structure of a bidispersed brush is characterized by the distinctive segregation of the free ends of longer and shorter chains. Shorter chains form a sublayer adjacent to the grafting surface while the end parts of longer chains form the periphery sublayer. Such segregation is provided by the strong stretching condition of both the shorter chains in the inner layer and the chain segments of the longer chains in the outer sublayer. This segregation leads to a kink in the monomer density profile. Unlike in the monodispersed case, the degree of stretching of the chains in a bidispersed brush is further governed by the relative composition of the long and short chains. If the fraction of short chains is small, the short chains behave as Gaussian coils stretched by an external field produced by the surrounding long chains[26] and their stretching is much less than that of a monodispersed brush composed only of short chains. On the other hand, for a small admixture of long chains, their peripherial chain parts form nonoverlapping coils "grafted" to the surface of the inner sublayer formed by the short chains. Hence one can expect that for given lengths of short and long chains SCF theory[19,20] will provide an adequate picture of a bidispersed brush only in a certain range of brush compositions. Within this range, both components of the brush are under the condition of strong stretching while outside this range, this condition breaks down. The aim of the present paper is to investigate the structure of a bidispersed brush for a wide range of brush compositions and chain lengths including the regions where the assumptions in the SCF theory are no longer valid. A brief Monte Carlo simulation investigation on the bidispersed brush was carried out by Chakrabarti and Toral[28] (using a different model) in which only one set of chain lengths and brush composition was studied and only the density profiles were calculated. The detailed characteristics of the bidispersed brush such as monomer density profiles, chain end distributions, chain trajectories, local bond orientations and moments of distributions of the

* To whom correspondence should be addressed. Present address: Institute of Physics, National Central University, Chung-Li, Taiwan 32054.

† Permanent address: Institute of Macromolecular Compounds, Academy of Science, St. Petersburg 199004, Russia.

0024-9297/92/2225-5201$03.00/0

long and short chains are obtained. These data are useful for a better understanding of the behavior of brushes in various regimes including relatively loose brushes where the SCF theory is expected to break down. The rest of this paper is organized as follows: In section 2 we summarize the results of analytical SCF theory[19,20] of bidisperse planar brushes in a good solvent, and some new analytic SCF results for the quantities measured in the simulations are derived. Section 3 gives some details about the simulations, section 4 presents the MC results and compares them with the theory, and finally, the paper is concluded in section 5.

2. Analytic SCF Results

In this section, we will list and derive the predictions of the analytic SCF calculations. We consider a bidisperse polymer brush consisting of short chains of length N_S and longer chains of length $N_L \geq N_S$. The chains are grafted onto an impermeable flat surface with surface coverage σ. The subscript L (S) will be used to denote quantities associated with the longer (shorter) chains. Let the relative difference in chain lengths be $\alpha = (N_L - N_S)/N_S$ and the fraction of longer chains in the layer be q. Under the conditions of considerable stretching with respect to Gaussian dimensions, a Newton approximation[7,10] can be applied, according to which polymer chains can be characterized by their "trajectories"—most probable paths determining the positions of all monomers.

Strong stretching of chains leads to the segregation of free ends of short and long chains, and as a result the bidisperse brush splits into two sublayers, as illustrated schematically in Figure 1. The layer closer to the wall of thickness H_S comprises the free ends of only shorter chains, while the outer sublayer of thickness $H_L - H_S$ consists of ends from the longer chains only. This picture of complete segregation of the two types of chain ends is only true in the infinitely long chain limit. For chain of finite lengths, there will be some interpenetrations. The excluded volume interactions between monomers in the brush can be described in terms of the self-consistent potential $U(z)$ which is related to the density of free energy of volume interactions $a^{-3}f[\phi(z)]$ via

$$U(z) = \delta f[\phi(z)]/\delta\phi(z) \tag{1}$$

where $\phi(z)$ is the volume fraction of polymer units at a distance z from the grafting plane. Assuming binary intermonomer interactions with $a^{-3}f = v\phi^2$, where v is the second virial coefficient and a^3 is the monomer volume, one obtains

$$\phi(z) = \frac{a^3}{2v}U(z) \tag{2}$$

The particular form of the potential $U(z)$ has been calculated in refs 19 and 20 to give

$$U(z) = \begin{cases} \dfrac{3\pi^2 H_o^2}{8pN^2a^2}(1 - (z/H_o)^2) & 0 \leq z \leq H_S \\ \dfrac{3\pi^2 H_o^2}{8pN^2a^2}(1 - u^2(z/H_o)) & H_S \leq z \leq H_L \end{cases} \tag{3}$$

where

$$u(x) = (x - \alpha[x^2 - (1-\alpha^2)(1-q^{2/3})]^{1/2})/(1-\alpha^2) \tag{4}$$

H_L and H_S are the brush heights of the longer and shorter chains respectively and H_0 is the brush height of the monodisperse chains of length N_S with the same coverage σ. p is the stiffness parameter of the chain. The brush heights are given by[20]

$$H_o = (8pv\sigma/\pi^2)^{1/3}N_S \tag{5}$$

$$H_S = H_o\sqrt{1 - q^{2/3}} \tag{6}$$

$$H_L = H_o(1 + \alpha q^{1/3}) \tag{7}$$

From eqs 2 and 3, the density profile of polymer units in the bidisperse brush has been obtained[19,20]

$$\phi(z) = \begin{cases} \dfrac{3}{2}\sigma^{2/3}\left(\dfrac{\pi^2a^3}{8pv}\right)^{1/3}(1 - (z/H_o)^2) & 0 \leq z \leq H_S \\ \dfrac{3}{2}\sigma^{2/3}\left(\dfrac{\pi^2a^3}{8pv}\right)^{1/3}(1 - u^2(z/H_o)) & H_S \leq z \leq H_L \end{cases} \tag{8}$$

Note that $\phi(z)$ has a discontinuous derivative at $z = H_S$. The total density profile $\phi(z)$ is composed of partial profiles of long and short chains, $\phi(z) = \phi_L(z) + \phi_S(z)$. The density profiles for the logn and short chains are

$$\phi_S(z) = \frac{3}{\pi}\sigma^{2/3}\left(\frac{\pi^2a^3}{8pv}\right)^{1/3}\left[q^{1/3}\sqrt{1 - q^{2/3} - (z/H_o)^2} + [1 - (z/H_o)^2]\tan^{-1}\left(\frac{\sqrt{H_S^2 - z^2}}{H_o q^{1/3}}\right)\right] \tag{9}$$

$$\phi_L(z) = \begin{cases} \phi(z) - \phi_S(z) & 0 \leq z \leq H_S \\ \phi(z) & H_S \leq z \leq H_L \end{cases} \tag{10}$$

The heights of the long and short chains can be characterized by the first moment of the density profiles. We obtain

$$\langle z\rangle_S = \frac{3H_o}{4\pi(1-q)}\left((q^{1/3} - 2q)\sqrt{1 - q^{2/3}} + \tan^{-1}\left[\frac{\sqrt{1-q^{2/3}}}{q^{1/3}}\right]\right) \tag{11}$$

$$\langle z\rangle_L = \frac{3H_o}{8q(1+\alpha)}\left(1 + \alpha q^{1/3} + \alpha q + \alpha^2 q^{4/3} + \frac{\alpha(1-q^{2/3})^2}{2}\ln\frac{1-q^{1/3}}{1+q^{1/3}}\right) - \frac{1-q}{q(1+\alpha)}\langle z\rangle_S \tag{12}$$

The distribution functions of the free ends of the long and short chains are given by[20]

$$g_L(z) = \frac{3\sqrt{1 - u^2(z/H_o)}}{q(1-\alpha^2)H_o}u(z/H_o) \times \left[1 - \frac{\alpha z}{\sqrt{z^2 - (1-\alpha^2)H_S^2}}\right] \quad H_S \leq z \leq H_L \tag{13}$$

$$g_S(z) = \frac{3z}{(1-q)H_o}\sqrt{H_o^2 - z^2} \quad 0 \leq z \leq H_S \tag{14}$$

The first moments of these distribution functions can be calculated to give

$$\langle z_L^e \rangle = \frac{3H_o}{8q}\left(\sin^{-1} q^{1/3} - q^{1/3}(1-2q^{2/3})\sqrt{1-q^{2/3}} + \frac{\alpha\pi}{2}q^{4/3}\right) \quad (15)$$

$$\langle z_S^e \rangle = \frac{3H_o}{8(1-q)}\left(\frac{\pi}{2} - \sin^{-1} q^{1/3} + q^{1/3}(1-2q^{2/3})\sqrt{1-q^{2/3}}\right) \quad (16)$$

The internal structure of the inner sublayer in a bidisperse brush coincides with that of a monodisperse brush of short chains with the same σ.[20] In particular, the trajectories of the shorter chains in a bidisperse brush are identical to those in a monodisperse brush of short chains, namely

$$z_S(i) = z_S^e \sin \gamma_i \quad (17)$$

where $z_S(i)$ is the position of the ith monomer, $z_S^e \equiv z_S(N_S)$ is the position of the free end, and $\gamma_i \equiv i\pi(2N_S)$. As for the trajectories of the long chains, they are determined by the following relationships. If the ith monomer of the longer chain is located in the inner sublayer ($z_L(i) \le H_S$), its position is given by

$$z_L(i) = H_o u(z_L^e/H_o) \sin \gamma_i \quad (18)$$

For the monomers located in the outer sublayer ($z_L(i) > H_S$), $z_L(i)$ is determined from the following equation:

$$\gamma_i = \sin^{-1}\left(\frac{z_L(i) - \alpha[z_L^2(i) - (1-\alpha^2)H_S^2]^{1/2}}{z_L^e - \alpha[z_L^{e\,2} - (1-\alpha^2)H_S^2]^{1/2}}\right) + \alpha \sin^{-1}\left(\frac{\alpha z_L(i) - [z_L^2(i) - (1-\alpha^2)H_S^2]^{1/2}}{\alpha z_L^e - [z_L^{e\,2} - (1-\alpha^2)H_S^2]^{1/2}}\right) \quad (19)$$

For the special case of $\alpha = 1$ (i.e. $N_L = 2N_S$), $z_L(i)$ can be solved explicitly from (19) to give

$$z_L(i) = \frac{1}{\sqrt{2}z_L^e}\sqrt{z_L^{e\,4} + H_S^4 - (z_L^{e\,4} - H_S^4)\cos\gamma_i} \quad (20)$$

The average trajectories for the long and short chains can then be obtained by integrating $z(i)$ with the appropriate end distributions g_S and g_L. We get

$$\langle z_S(i) \rangle = \langle z_S^e \rangle \sin \gamma_i \quad \text{for all } \alpha \quad (21)$$

And for $\alpha = 1$, $\langle z_L(i) \rangle$ is

$$\frac{3H_o}{8q}(\sin^{-1} q^{1/3} - q^{1/3}(1-2q^{2/3})\sqrt{1-q^{2/3}}) \sin \gamma_i \qquad z^* > H_L$$

$$\int_{z^*}^{H_L} dz_L^e\, g_L(z_L^e) z_L(i) + \frac{3H_o}{8q}(\sqrt{1-q^{2/3}}[(q^{2/3} - \cos^2\gamma_i) \times (1-2q^{2/3} + \cos^2\gamma_i)\csc^4\gamma_i - q^{2/3}(1-2q^{2/3})] + [1 - q^{2/3} + q^{1/3}\sqrt{q^{2/3} - \cos^2\gamma_i}]\csc\gamma_i) \qquad H_S < z^* < H_L \quad (22)$$

$$\int_{H_S}^{H_L} dz_L^e\, g_L(z_L^e) z_L(i) \qquad z^* < H_S$$

where $z^* = H_S(\cot\gamma_i + \csc\gamma_i)$ and $z_L(i)$ is given by eq 20. The orientation of the ith bond $\langle \cos\theta_i \rangle$ induced by grafting can also be calculated

$$\langle \cos\theta_i \rangle \equiv \left\langle \frac{z(i) - z(i-1)}{|\vec{r}(i) - \vec{r}(i-1)|} \right\rangle = \frac{\langle z(i) \rangle - \langle z(i-1) \rangle}{\langle l^2 \rangle^{1/2}} \quad (23)$$

where $\langle l^2 \rangle^{1/2}$ is the bond length between consecutive monomers along a chain. When the monomer positions are known from eqs 21 and 22, $\langle \cos\theta_i \rangle$ for the long and short chains can be obtained easily.

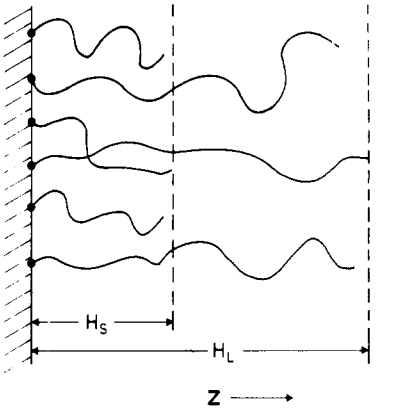

Figure 1. Schematic picture for the bidisperse grafted polymer layer.

3. Some Simulation Details

The bond-fluctuation model[40-43] of polymer chains on lattices is used in the simulations. In this model, each effective monomer occupies eight neighboring lattices of a simple cubic lattice. Self-avoidance is modeled by the requirement that no two monomers can have a common site. Thus, $a = 2$ should be used in analyzing the MC data. The 108 allowed bond vectors connecting two successive monomers are obtainable from the set {(2, 0, 0), (2, 1, 0), (2, 1, 1), (2, 2, 1), (3, 0, 0), and (3, 1, 0)} by the symmetry operations of the cubic lattice, and the bond lengths range from 2 to $\sqrt{10}$ lattice spacings and are characterized by the root-mean-square bond length $\langle l^2 \rangle^{1/2}$. In the range of concentration in this study, $\langle l^2 \rangle^{1/2} \simeq 2.71 \pm 0.2$. The MC procedure starts by choosing a monomer at random and trying to move it one lattice spacing in one of the randomly selected directions: $\pm x$, $\pm y$, $\pm z$. The move will be accepted only if both self-avoidance is satisfied and the new bonds still belong to the allowed set. The choice of this set of bond vectors guarantees that no two bonds will cross each other in the course of their motions and thus entanglement is automatically taken care of. Hence this model is especially suitable for studying multichain systems. This model has been used in a previous MC study[29,30] of monodispersed grafted polymer chains in a good solvent. The parameters of this model such as the excluded volume interaction parameter v and the stiffness parameter p of the chains are known[30] which are essential for a detailed quantitative comparison with the theory. And it has been demonstrated[30] in the monodispersed brushes that the MC results are well described by the SCF theory. From our previous study of the monodisperse brush[30] using the bond-fluctuation model, we have $vp \simeq 31.2$ and this value will be used in analyzing the present data.

Our system consists of polymer chains of two different lengths, N_L and N_S for the longer and shorter chains, respectively. One end of each chain is grafted irreversibly on an impenetrable $L \times L$ surface (xy plane), and the chains are placed inside a $L \times L \times 3N_L + 1$ box so that the other nongrafted surface never restricts the chain configurations. The grafting sites are selected randomly but are strictly self-avoiding on the grafting surface. Periodic boundary conditions are imposed in the x and y directions. There are no monomer–monomer and monomer–wall interactions apart from self-avoidance so as to model the good solvent situation. The starting configu-

Table I
Table of MC Results for the First Moments of Concentration Profiles, First Moments of Distribution of Free Ends, and Brush Heights for Long and Short Components for Various Chain Lengths and Coverages[a]

	N_L	N_S	σ	q	α	$\langle z\rangle_L$	$\langle z\rangle_S$	$\langle z_L^e\rangle$	$\langle z_S^e\rangle$	H_L	H_S
a	40	20	0.1	0.5	1.0	21.50	8.93	34.11	13.48	52.0	15.0
b	60	30	0.1	0.5	1.0	31.43	13.27	51.34	19.68	71.0	23.5
c	80	40	0.1	0.5	1.0	41.56	16.82	66.30	26.67	95.0	31.0
d	60	20	0.1	0.5	2.0	30.00	8.97	46.95	13.69	72.0	15.0
e	60	40	0.1	0.5	0.5	33.66	16.56	54.13	25.85	76.0	31.0
f	40	20	0.05	0.75	1.0	17.01	7.88	26.05	11.68	42.0	7.0
g	40	20	0.1	0.75	1.0	21.00	7.52	33.54	10.98	54.0	11.5
h	40	20	0.15	0.75	1.0	24.25	8.35	39.35	12.47	58.0	13.5
i	40	20	0.05	0.25	1.0	17.40	8.74	26.78	13.19	40.0	12.5
j	40	20	0.1	0.25	1.0	21.39	9.92	32.71	15.43	46.0	17.5
k	40	20	0.15	0.25	1.0	24.62	11.02	37.80	17.49	52.0	22.0

[a] The uncertainties for the first moments are about 5%, and those of the brush heights are about 10%.

rations are allowed to equilibrate for a long time, typically 5 times the relaxation time of a monodisperse brush of length N_L with the same surface coverage. The relaxation times of monodisperse brushes were known[29] from previous studies and hence we are confident that our systems have been well equilibrated. Then statistical samples were taken from runs extending over a long period of time (typically several times of the equilibration time). In this simulation, we choose $L = 40$, $40 \le N_L \le 80$ and $20 \le N_S \le 40$. As has been noticed in the previous study of monodisperse brushes, scaling behavior can already be observed with chain lengths ≥ 20. The surface coverage σ in this study ranges from $0.05 \le \sigma \le 0.15$.

4. Monte Carlo Results and Discussion

Table I lists the chain lengths, the fraction of longer chains, q, and the relative excess length, α, considered in the simulations. Also shown in the table are the MC data for the first moments of the density profiles and end distributions for the long and short chains. The brush heights for the long and short components are also estimated from the data. H_S is estimated from the distance at which $\phi(z)$ deviates from the profile of a monodisperse brush of length N_S with the same coverage, as implied in eq 8. H_L is estimated from $\phi(H_L) = 0$. H_0 is obtained from the SCF result in eq 5. To test the dependences on the parameters q and α as given by the SCF theory, we plot in Figure 2a the reduced brush heights as a function of q for the data with $\alpha = 1$. The solid lines are the predictions from (6) and (7) which show reasonable agreement except for the data with $\sigma = 0.05$ and $q = 0.25$. This is due to the fact that at this relatively low coverage and small number of longer chains, the chains in the outer sublayer are not stretched enough to be in the brush regime and hence the SCF theory does not apply in this case. Similarly in Figure 2b, the reduced first moment of the distributions of free ends are plotted as a function of α for the $q = 0.5$ data. $\langle z_L^e\rangle$ increases linearly with α and is nicely confirmed by the MC data. $\langle z_S^e\rangle$ is predicted to be independent of α, and this is also observed in our data. But the MC data are systematically slightly larger than the SCF predictions (horizontal solid line); this is due to the penetration of the free ends of the short chains into the outer sublayer due to the finite (and relatively short, $N_S = 20$) length of the chains. This penetration makes $\langle z_S^e\rangle$ somewhat larger than predicted from theory.

Figure 3 shows the density profiles for the bimodal brush with $N_S = 20$ and $N_L = 40$ and 60. The monodisperse brush with $N = 20$ and the same coverage is also included for comparison. The profile for the monodisperse chains coincides with that of the bidisperse brushes up to $z \simeq H_S$, as predicted in the SCF theory. The total density

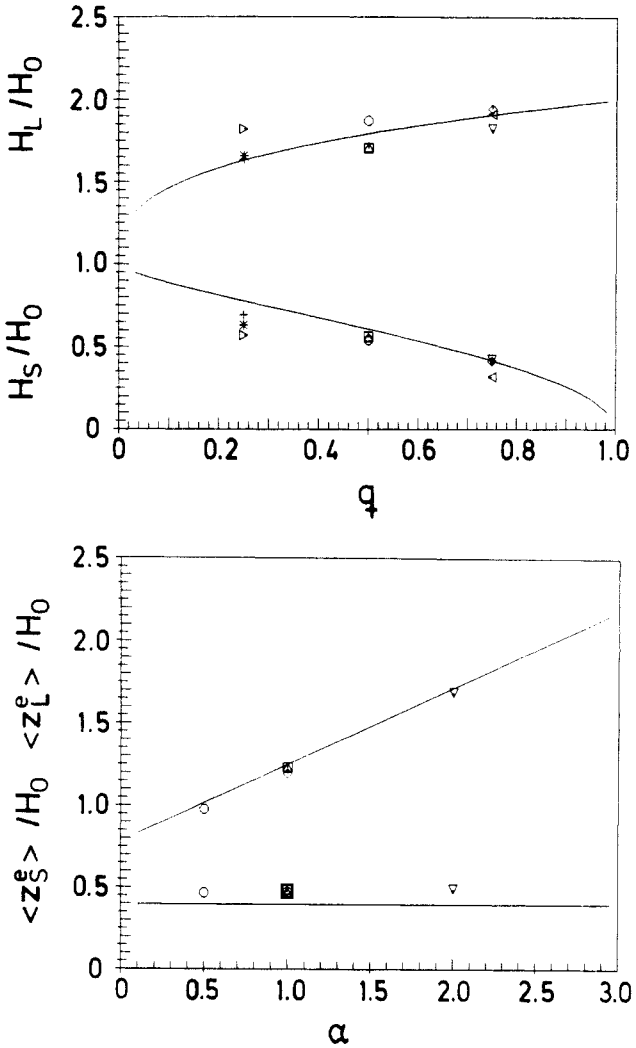

Figure 2. (a, Top) H_L/H_0 (upper part of data) and H_S/H_0 (lower part) versus q for the data with $\alpha = 1$. The data are labeled with the notations in Table I. Symbols: (○) a; (□) b; (△) c; (<) f; (◇) g; (▽) h; (>) i; (*) j; (+) k. The solid lines are the SCF results from eqs 6 and 7. (b, Bottom) $\langle z_L^e\rangle/H_0$ (upper part of data) and $\langle z_S^e\rangle/H_0$ (lower part) versus α for th data with $q = 0.5$. Symbols: (○) e; (□) a; (△) b; (◇) c; (▽) d. The solid lines are the SCF results from eqs 15 and 16.

$\phi(z)$ for the bimodal brush shows a clear discontinuous first derivative around $z \sim H_S$, as predicted by the SCF theory. This "kink" is more prominent as N_L gets longer at fixed σ. When compared to a previous Monte Carlo simulation of bidisperse brushes using another model,[28] the singularity in $\phi(z)$ is observed more convincingly in the present model even for much smaller values of N_L and N_S. This rapid approach to the asymptotic behavior has

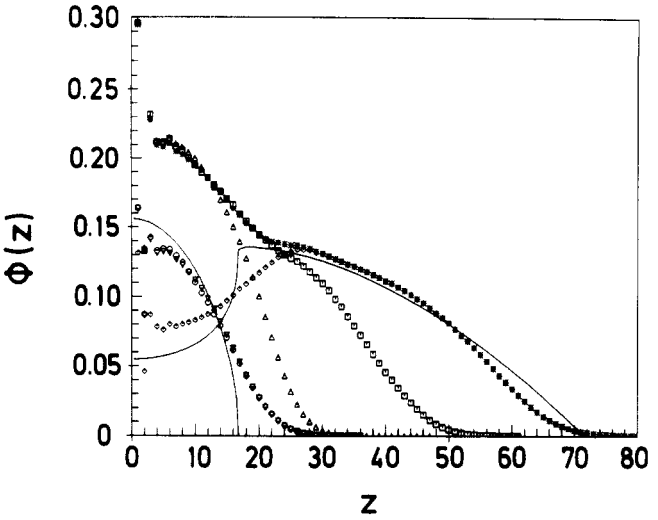

Figure 3. Density distributions for brushes with $N_S = 20$ and $\sigma = 0.1$. Symbols: (○) ϕ_S in a; (□) ϕ in a; (△) ϕ for the monodisperse brush; (◇) ϕ_L in d; (▽) ϕ_S in d; (*) ϕ in d. The solid curves are the SCF results for ϕ_S and ϕ_L in d.

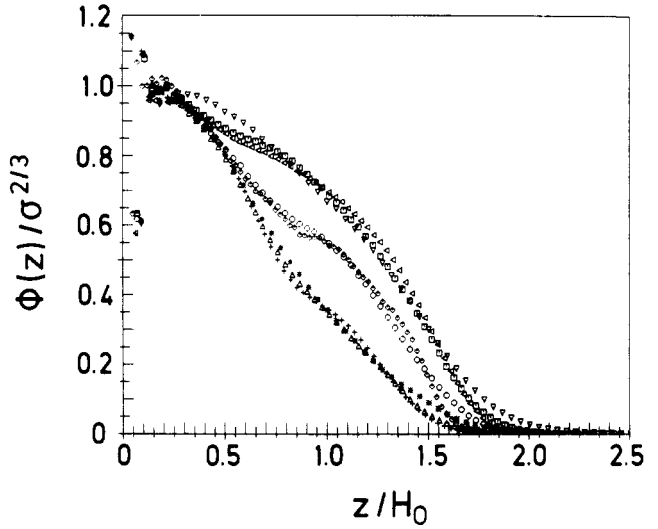

Figure 4. Scaling plot for the density profiles for data with $\alpha = 1$ and $q = 0.25$ (upper set of data), 0.5 (middle), and 0.75 (lower). Symbols: (○) a; (□) g; (△) i; (<) h; (◇) b; (▽) f; (+) k.

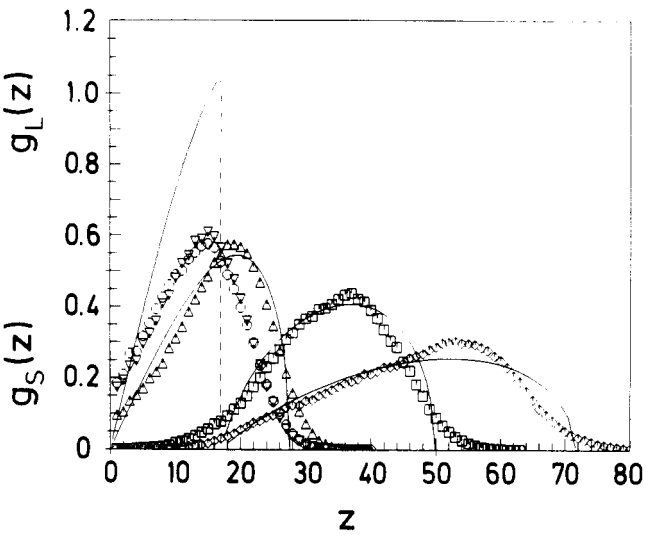

Figure 5. Free end distributions for brushes with $N_S = 20$ and $\sigma = 0.1$. Symbols: (○) g_S in a; (□) g_L in a; (△) end distribution for the monodisperse brush; (◇) g_L in d; (▽) g_S in d. The solid curves are the corresponding SCF results. The dashed vertical line is just a guide to the eye.

been noted in other applications of the bond-fluctuation model.[42,43] The profiles for the long and short components are also shown. The $\phi_S(z)$'s are identical for different lengths of the longer chains. This confirms the result from SCF theory that the increase in the length of the longer chains does not affect the short chains. As can be seen in the previous section, all the "short" quantities ($\phi_S(z)$, $g_S(z)$, etc.) do not depend on α (and hence N_L). Finally, the analytical SCF predictions for $\phi_L(z)$ and $\phi_S(z)$ are also plotted (solid curves) on the same figure; they show reasonable agreement with the MC data. Figure 4 is a scaling plot with $\phi(z)\sigma^{-2/3}$ versus z/H_0 as suggested by eq 8. The data shown are for $\alpha = 1$ with $q = 0.25$, 0.5, and 0.75 corresponding to the three sets of collapsing data. More careful observation reveals that data set i (the data sets are labeled as in Table I) does not scale well, again due to the chains in the outer sublayer which are not in the stretched brush regime.

The interpenetration of the free ends of longer chains in the inner sublayer and vice versa for free ends of short chains in the outer sublayer can be seen explicitly in their end distribution functions. Figure 5 displays $g_L(z)$ and $g_S(z)$ for $N_S = 20$ and $N_L = 40$ and 60. The end distribution for the monodisperse chains of length N_S with the same coverage are also shown. The corresponding analytical SCF results are also shown (solid curves). SCF theory assumes the long chain length limit and predicts a complete segregation of long and short chain ends. Our MC data for finite chain lengths indicate significant chain end interpenetrations. The penetration of the short ends into the outer sublayer is more than that of the long ends into the inner sublayer. This is because the maximum of $g_S(z)$ is located close to the boundary between the two sublayers. Hence a considerable amount of shorter chain ends are able to penetrate into the outer layer. On the contrary $g_L(z)$ peaks far from this boundary and only a small fraction of longer chain ends is located in the vicinity of the boundary. Hence penetration of longer chains into the inner layer is less probable and decreases with increasing N_L. As shown in the figure, the distributions of the short chains are identical for $N_L = 40$ and 60, again verifying that the properties of the shorter chains are independent of the value of N_L as long as $N_L - N_S \gg 1$. The agreement with the SCF results for $g_L(z)$ is quite good but is less satisfactory for $g_S(z)$. This is due to the penetration of the ends into the outer layer, and since the distribution is normalized such that the area under the curve $g_S(z)$ is unity, the MC data look much lower than the SCF prediction. Another observation worth mentioning is that $g_S(z)$ for the bidisperse brush peaks at a smaller z when compared to the end distribution of a monodisperse brush of the same length and coverage. This can be understood as follows: In the presence of longer chains, the portions of longer chains in the outer sublayer are less crowded and hence it is more favorable for the longer chains to have more polymer units in the outer layer. This is also verified in Figure 3 for the $\phi_L(z)$ data which show a maximum at $z > H_S$. Thus the portion of long chain in the inner sublayer is more stretched, making more room for the shorter chains, and thus short chains are less stretched when compared to the monodisperse brush. This can be visualized explicitly in Figure 6 which shows a snapshot of the chain configurations in a bidisperse brush. For the purpose of a clear visualization of the chain configurations, only one long and one short chain are displayed (out of a total number of 40 chains at $\sigma = 0.1$). As shown in the figure, the portion of the longer chain in the inner sublayer is more stretched than the portion in the outer sublayer. Also the shorter chain is less stretched compared

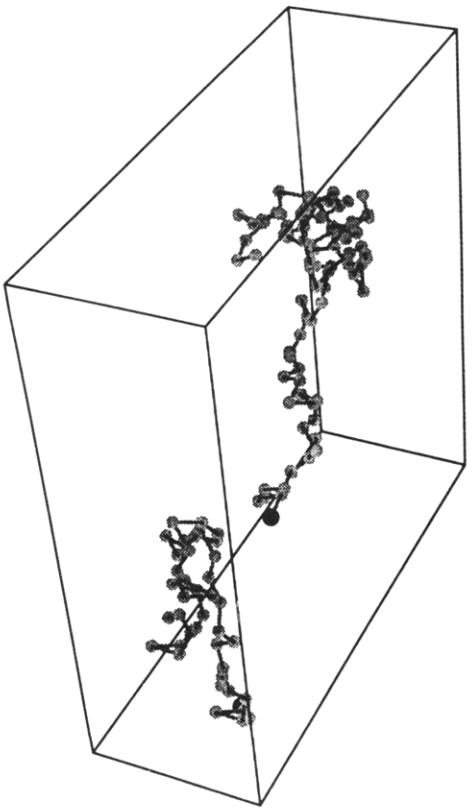

Figure 6. Snapshot of the equilibrium chain configurations of the long and short chains with $\sigma = 0.1$, $N_L = 80$, and $N_S = 40$ (data c in Table I). Only one short and one long chain are shown for clarity purpose. The bottom plane is the grafting surface. The grafted monomers are solid and the others are shaded.

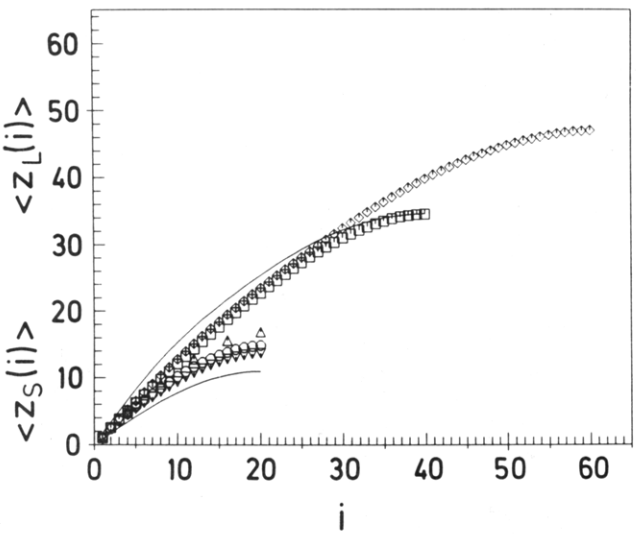

Figure 7. Average position of the ith monomer for brushes with $N_S = 20$ and $\sigma = 0.1$. Symbols: (○) $\langle z_S(i)\rangle$ in a; (□) $\langle z_L(i)\rangle$ in a; (△) $\langle z(i)\rangle$ for the monodisperse brush; (◇) $\langle z_L(i)\rangle$ in d; (▽) $\langle z_S(i)\rangle$ in d. The solid curves are the SCF results corresponding to a.

with the portion of longer chain in the inner layer.

The average trajectories of the long and short chains are shown in Figure 7 for $N_S = 20$ and $N_L = 40$ and 60. The data for the monodisperse brush are also displayed. Again the data for the short chains are almost the same for different values of N_L. Also, for the longer chains, the monomer positions for the two different N_L's are very close, except near the brush end. The positions of the monomers of the shorter chains are closer to the wall when compared to that of the corresponding monodisperse

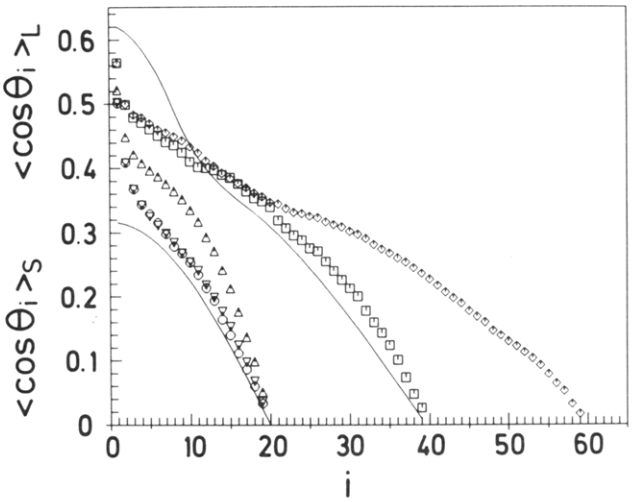

Figure 8. Plot of the projection $\langle\cos\theta_i\rangle$ of the local orientation vector of bond-connecting monomer $i-1$ and i vs the position of the ith bond along the chain for brushes with $N_S = 20$ and $\sigma = 0.1$. Symbols: (○) $\langle\cos\theta_i\rangle_S$ in a; (□) $\langle\cos\theta_i\rangle_L$ in a; (△) $\langle\cos\theta_i\rangle$ for the monodisperse brush; (◇) $\langle\cos\theta_i\rangle_L$ in d; (▽) $\langle\cos\theta_i\rangle_S$ in d. The solid curves are the SCF results corresponding to a.

brush; this again confirms the picture that in the presence of longer chains, the short chains are less stretched compared to the monodisperse case. The SCF results from eqs 21 and 22 (solid curves) show a noticeable discrepancy for the short chain data. The discrepancy is due to the fact that SCF theory predicts no interpenetration which would underestimate the monomer distance from the wall for the short chains of finite length. The singularity implied from the SCF result for $\langle z_L(i)\rangle$ is not visually prominent in the plot. This singularity is more outstanding visually in the data for $\langle\cos\theta_i\rangle$ in Figure 8. The orientation of the bonds induced by grafting is displayed for the brushes of the same lengths as in Figure 7. The SCF results for the $N_L = 40$ and $N_S = 20$ data (solid curves) from eqs 21–23 are shown; the value of the root-mean-square bond length in (23) is taken to be $\langle l^2\rangle^{1/2} \simeq 2.71$ from our simulation data. For the longer chains, the SCF result shows the curvature changes sign twice. This is also observed in the MC data, and the effect is more prominent in the longer N_L data. For the short chains, we see once again the data are identical for the two values of N_L. When compared to the monodisperse brush of length N_S, the bonds of the short polymers are less aligned perpendicular to the wall, again verifying the picture that the short chains have more room and hence are less stretched while the portions of long chains in the inner sublayer are more stretched.

5. Conclusions

We present Monte Carlo results for the bimodal disperse polymer brushes and compare them with the analytical SCF predictions. We found that the structure of a bidisperse brush is adequately described by the SCF results when both the short and long chains are stretched. The singularities predicted in the theory are observed in the data although they are somewhat smoothed out due to the finite chain lengths. The dependence of the brush thickness on the fraction of longer chain q and the relative excess length α agree reasonably well with the SCF predictions except for data with smaller values of q in which the portion of chains in the outer layer is not stretched. Also the structural properties of the short chains depend very little on the lengths of the longer chains, agreeing with the SCF predictions. The SCF prediction

is less satisfactory for the distribution functions, especially the end distribution of the short chains, $g_S(z)$. The discrepancies are predominantly due to interpenetration of the free ends into the other sublayers. We also confirmed from the data the picture that the portion of the long chains in the inner sublayer is more stretched compared to their short chain counterpart and the short chains have more lateral room and are less stretched compared to the monodisperse brush of the same length and coverage.

In general, the agreement with the SCF theory is not as good as in the case of monodisperse brushes.[30] In the monodispersed brush with moderate coverage, MC results already approach the asymptotical SCF predictions for $N \simeq 20$–30, while in the bidispersed brush SCF predictions are in reasonable agreement only for higher values of N_S and in the intermediate range of brush compositions. Increasing the chain lengths of the grafted chains at fixed σ would increase the stretching of the chain, and thus one expects a better agreement with the analytical SCF predictions for a wider range of brush compositions.

Acknowledgment. This research is supported by the Bundesministerium für Forschung und Technolgie (BMFT) Grant No. 03M4040. E.B.Z. acknowledges support from the Alexander von Humboldt Foundation. We thank Prof. K. Binder for a critical reading of the manuscript.

References and Notes

(1) Halperin, A.; Tirrell, M.; Lodge, T. P. *Adv. Polym. Sci.* **1991**, *100*, 31.
(2) Milner, S. T. *Science* **1991**, *251*, 905.
(3) Alexander, S. *J. Phys. (Paris)* **1977**, *38*, 983.
(4) de Gennes, P. G. *C. R. Hebd. Seances Sci.* **1985**, *300*, 839; *Macromolecules* **1980**, *13*, 1069.
(5) Cosgrove, T.; Heath, T.; van Lent, B.; Leermakers, F.; Scheutjens, J. *Macromolecules* **1987**, *20*, 1692.
(6) Marques, C.; Joanny, J. F.; Leibler, L. *Macromolecules* **1988**, *21*, 1051.
(7) Milner, S.; Witten, T.; Cates, M. *Macromolecules* **1988**, *21*, 2610; *Europhys. Lett.* **1988**, *5*, 413.
(8) Milner, S. *Europhys. Lett.* **1988**, *7*, 695.
(9) Munch, M. R.; Gast, A. P. *Macromolecules* **1988**, *21*, 1366.
(10) Skvortsov, A. M.; Gorbunov, A. A.; Pavlushkov, I. E.; Zhulina, E. B.; Borisov, O. V.; Priamitsyn, V. A. *Polym. Sci. USSR* **1988**, *30*, 1706.
(11) Zhulina, E. B.; Borisov, O. V.; Priamitsyn, V. A. *J. Colloid Interface Sci.* **1990**, *137*, 495; *Polym. Sci. USSR* **1989**, *31*, 205; *Polym. Sci. USSR* **1984**, *26*, 885.
(12) Birshtein, T. M.; Zhulina, E. B. *Polym. Sci. USSR* **1983**, *25*, 2165.
(13) Zhulina, E. B.; Borisov, O. V. *J. Colloid Interface Sci.* **1991**, *144*, 507.
(14) Zhulina, E. B.; Borisov, O. V.; Brombacher, L. *Macromolecules* **1991**, *24*, 4679.
(15) Miklavic, S. J.; Marcelja, S. *J. Phys. Chem.* **1988**, *92*, 6718.
(16) Mirsra, S.; Varanasi, S.; Varanasi, P. P. *Macromolecules* **1989**, *22*, 4173.
(17) Zhulina, E. B.; Borisov, O. V.; Birshtein, T. M. *J. Phys. II* **1992**, *2*, 63.
(18) Muthukumar, M.; Ho, S. *Macromolecules* **1898**, *22*, 965.
(19) Milner, S.; Witten, T.; Cates, M. *Macromolecules* **1989**, *22*, 853.
(20) Birshtein, T. M.; Liatskaya, Yu V.; Zhulina, E. B. *Polymer* **1990**, *31*, 2185.
(21) Tirrell, M.; Parsonage, E. E.; Watanabe, H.; Dhoot, S. *Polym. J.*, in press.
(22) Shim, D. F. K.; Cates, M. E. *J. Phys. (Paris)* **1989**, *50*, 3535.
(23) Lai, P.-Y.; Halperin, A. *Macromolecules* **1991**, *24*, 4981.
(24) Marko, J. F.; Witten, T. A. *Phys. Rev. Lett.* **1991**, *66*, 1541.
(25) Halperin, A.; Alexander, S. *Europhys. Lett.* **1988**, *6*, 329; *Macromolecules* **1989**, *22*, 2403.
(26) Klushin, L. I.; Skvortsov, A. M. *Macromolecules* **1991**, *24*, 1549.
(27) Murat, M.; Grest, G. S. *Macromolecules* **1989**, *22*, 4054; *Phys. Rev. Lett.* **1989**, *63*, 1074.
(28) Chakrabarti, A.; Toral, R. *Macromolecules* **1990**, *23*, 2016.
(29) Lai, P.-Y.; Binder, K. *J. Chem. Phys.* **1991**, *95*, 9288 (in *Proceedings of the International Conference on Polymer-Solid Interfaces*; Adam Hilger: Bristol, PA, 1992; p 371.
(30) Lai, P.-Y.; Zhulina, E. B. *J. Phys. II* **1992**, *2*, 547.
(31) Cosgrove, T.; Crowly, T.; Vincent, B. In *Adsorption from Solutions*; Otterwill, R., Rochester, C., Smith, A., Eds.; Academic Press: New York, 1982; p 287.
(32) Edwards, J.; Lenon, S.; Toussaint, A.; Vincent, B. In *Polymer Adsorption and Dispersion Stability*; ACS Symposium Series 240; American Chemical Society: Washington, DC, 1984.
(33) Hadzioannou, G.; Patel, S.; Granick, S.; Tirrell, M. *J. Am. Chem. Soc.* **1986**, *108*, 2869.
(34) Luckham, P. F.; Klein, J. *J. Colloid Interface Sci.* **1987**, *54*, 286.
(35) Ansarifar, A.; Luckham, P. F. *Polymer* **1988**, *29*, 329.
(36) Taunton, H. J.; Toprakcioglu, C.; Fetters, L. J.; Klein, J. *Nature* **1988**, *332*, 712; *Macromolecules* **1990**, *23*, 571.
(37) Taunton, H. J.; Toprakcioglu, C.; Klein, J. *Macromolecules* **1988**, *21*, 3333.
(38) Auroy, P.; Auvray, L.; Leger, L. *Phys. Rev. Lett.* **1991**, *66*, 719.
(39) Zhao, X.; Zhao, W.; Rafailovich, M. H.; Sokolov, J.; Russell, T. P.; Kumar, S. K.; Schwarz, S. A.; Wilkins, B. J. *Europhys. Lett.* **1991**, *15*, 725.
(40) Carmesin, I.; Kremer, K. *Macromolecules* **1988**, *21*, 2819; *J. Phys. (Paris)* **1990**, *51*, 915.
(41) Deutsch, H.-P.; Binder, K. *J. Chem. Phys.* **1991**, *94*, 2294.
(42) Paul, W.; Binder, K.; Heermann, D. W.; Kremer, K. *J. Phys. II* **1991**, *1*, 37; *J. Chem. Phys.* **1991**, *95*, 7726.
(43) Deutsch, H.-P.; Dickman, R. *J. Chem. Phys.* **1990**, *93*, 8983.